Egypt. J. Chem. **Vol. 66**, No. SI: 13 pp. 117 - 126 (2023)

Egyptian Journal of Chemistry

http://ejchem.journals.ekb.eg/

Coupling of SEM-EDX and Raman Spectroscopy to Investigate Painted Preparation Layers on Two Wooden Statuettes from Ptolemaic Era

Kareem M.E. Hamouda[*a], Nesrin M.N. El Hadidi [b], Safa A.M. Hamed [* b], Mohamed S. Abdel-Aziz [c].

[a] *Conservation Department, General Administration for the Restoration of Antiquities and Museums of East Delta, Ministry of Tourism and Antiquities, Sharkia, Egypt*

[b] *Conservation Department, Faculty of Archaeology, Cairo University, Giza, Egypt*

[c] *Microbial Chemistry Department, National Research Centre, Giza, Egypt*

Abstract

Multi-analytical techniques combining SEM-EDX and Raman spectroscopy have been employed in this study to investigate the chemical composition of the preparation layers and pigments applied on two wooden statuettes of the goddess Isis from the Ptolemaic era preserved in Tell Basta's museum storeroom. Furthermore, light microscope was used to identify wood species in both statuettes and FTIR analysis to identify the binding media. Results proved that both statuettes were made of local wood; statuette no. 1408 was carved out of tamarisk wood, while statuette no. 2213 was made of sycamore fig. Preparation layer applied on statuette no. 1408 was predominantly composed of calcium carbonate and gypsum and the statuette no. 2213 was made with calcium carbonate. EDX coupled with Raman results indicate that the pigments used were mostly in accordance with the established Ancient Egyptian palette.

Keywords: Isis's wooden statuettes; pigments; optical microscope, SEM-EDX; FTIR; Raman spectroscopy.

1. Introduction

Two wooden statuettes of the goddess Isis dating back to the Ptolemaic era were found in *Al-Sowwah* excavation site near Sharkia, Egypt in 1995. In the Abu Hammad region, where Petri and Duncan collaborated in 1906, the latter made every effort to excavate parts of the *Al-Sowwah* region in order to connect it with nearby archaeologically significant locations, such as *Saft al-Hanna* (*Bar-Sibdo*) and *Tell Basta* (*Bar-Bastet*). The Liverpool University's mission, which examined and studied the area in 1986, supported the Egyptian Antiquities Authority's claim that burial in the *Al-Sowwah* region began at the end of the Eighteenth Dynasty and continued until the Roman era. It was mentioned that the necropolis of the capital of the twentieth district of Lower Egypt is located in the areas of *Al-Sowwah, Al-Khalwa, Al-Sheikh Dhikra*, and *Kafr Abu Al-Nour*. A large number of tombs, and numerous ancient artifacts were discovered there, including papyrus, amulets, *Ushabtis*, pottery, and painted gesso masks, stone, pottery, and wooden coffins (1).

The wooden statuettes listed under nos. 1408 and 2213 are currently kept in *Tell Basta*'s museum storeroom. The first one is of Isis in a devotional position, it is 36.5 cm long and is missing an arm and other body parts (Figure 1a). The second one depicts Isis in a seating position with both arms and portions of the base missing. It measures 32 cm in length and has a 9.5 x 8.5 cm base (Figure 1b). Both statuettes are covered with a painted layer with various

*Corresponding author e-mail: archaeo.kareem@gmail.com. (Kareem Mohamed Elsayed Hamouda); Safa_hamed@cu.edu.eg (Safa Abdelkader Mohamed Hamed).

EJCHEM use only: Received date: 05 January 2023; revised date 27 February 2023; accepted date 05 March 2023

DOI: 10.21608/EJCHEM.2023.184885.7411

©2023 National Information and Documentation Center (NIDOC)

pigments applied on a preparation layer. Statuette no. 1408 had preparation layer painted with black, red, white, in addition to a gilding layer, while statuette no. 2213 had a preparation layer painted with black, red, and blue pigments. Both statuettes displayed the basic colour palette typical of Egyptian art (2). These statuettes look very similar to most of the artifacts of that time, imitating Middle Kingdom styles. Additionally, during this period, kneeling figures of Isis and Nephthys began to be placed on either side of the sarcophagus in the burial chambers of private tombs (3).

Extensive research has been done on the pigments and binders used during the Egyptian periods. This era's colors were either synthetic or natural pigments made from finely powdered materials (4&5).

Natural pigments used by the ancient Egyptians were prepared by them, and synthetic pigments have been utilized historically since the Dynastic Period. They included the well-known Egyptian blue and arsenic sulfides such as realgar (As_4S_4) and orpiment (As_2S_3) (6&7).

The conventional stratigraphy of painted fragments on Egyptian artefacts consisted of a preparation layer that acted as a substrate support and one (or two, if there was overlap in the motifs) paint layer that was applied on it. Typically, the preparation layer was composed of gypsum, lime, or a combination of the two in mural paintings dating back to the Ptolemaic period (5). The same layers were usually used in polychrome wood.

On Egyptian artefacts, pigments were frequently applied using the tempera painting technique. To achieve adhesion between the pigment grains, the pigment was blended with a water-soluble binding agent, such as protein- and polysaccharide-based compounds (8&9).

Animal glue, eggs, and casein are a few examples of protein-based materials that would have been available to the Egyptians (8), and egg yolk has been identified in wooden coffins dating to the Ptolemaic period in Egypt (10).

The aim of the current study is to identify and compare wood species, preparation layer, and painted layer of the two wooden statuettes of Isis. SEM-EDX and Raman spectroscopy were used to investigate painted preparation layers on these statuettes.

Figure 1a, b: Represents the two wooden statuettes of goddess Isis from Ptolemaic era

2. Material and methods

2.1. Sampling

The painted fragments which had fallen off from the wooden statuettes nos. 2213 and 1408 were investigated and analyzed to identify and compare wood species, the preparation layer composition, the binding media, and pigments applied on the two statuettes.

2.2. Light Microscope

A light microscope (Leica -ICC 50 – HD) was used to identify the wood species of the two wooden statuettes. Semi-thin sections of samples were cut with a glass knife using a microtome into three directions: transverse section (TS), tangential longitudinal section (TLS) and radial longitudinal section (RLS). Stained sections were observed and photographed.

2.3. ESEM-EDX microanalysis

SEM study was performed to study painted preparation layer samples by fixing small pieces of an appropriate size on aluminium stubs with double-sided cellophane tape. The samples were examined using a Quanta250 FEG SEM. For pigments identification, the elemental composition of the various paint layers was analysed using an EDX unit attached to SEM**.** Three spots for each painted sample were analysed to obtain the mean values.

2.4. Fourier Transform Infra-Red Spectroscopy (FTIR)

FTIR was used to investigate the binding media which was used in the painted preparation layers. Samples were analysed with a FTIR spectrometer (Model 6100 Jasco, Japan). Spectra were obtained in the transmission mode with TGS detector using KBr method and represent (2mm/sec) co-added scans at the spectral region ranging from 400 cm^{-1} to 4000 cm^{-1}. It was identified by comparing the obtained spectra with literature data (11) and standards at the FTIR laboratories.

2.5. Raman spectroscopy

Painted samples were analysed to confirm SEM-EDX results of the pigments using a Senterra Raman spectrometer (Bruker) with a 20× objective lens and 785 nm lasers with 5-20 second integration times and 1-10 mW power. Spectra were recorded from 0 to 4000 cm^{-1}. Raman spectra were subjected to baseline correction and smoothed.

2.6. Statistical analysis

The elemental composition of the painted preparation layer samples was analysed using SPSS (version 25, IBM, Inc.). For all measures, the significance is set at an alpha level of 0.05 and the data are presented as means and standard deviations (SDs).

3. Results and discussion

3.1. Identification of wood

Microscopic investigation indicated that the wood used in the wooden statuette (no.1408) was identified as Tamarisk (*Tamarix* sp. L.), where the diagnostic features (Fig. 2) revealed that the transversal section's (TS) anatomical features included semi-ring porous to diffuse porous wood, solitary and clustered vessels, and sparse paratracheal to vasicentric axial parenchyma. Tangential longitudinal section revealed simple perforation plates and multiseriate rays (5–12 cells) in width (TLS). Heterocellular rays with procumbent, square, and upright cells interspersed throughout the ray were seen in the radial longitudinal section (RLS). It is stated that the tamarisk wood is indigenous to Egypt and is derived from tiny trees (12). Regarding the other wooden statuette (no. 2213), the wood utilized was sycamore fig (*Ficus sycomorus*) (Fig. 3). Diffuse porosity, solitary or in radial multiples of 2 to 4, and axial parenchyma vasicentric in bands more than three cells broad as seen in TS were employed as diagnostic features to identify *Ficus sycomorus* L. Prismatic crystals in non-chambered axial parenchyma cells, rays of two unique sizes, 1-4 seriate and bigger rays typically 5 to 12 seriate up to 20 high, and some lacticifers were detected in rays as seen in TLS. Heterocellular rays having core cells that are strongly procumbent and only have square, upright cells on marginal rows; simple perforation plates and solitary prismatic crystals present in upright and / or square ray cells as seen in RLS (13&14&15&16).

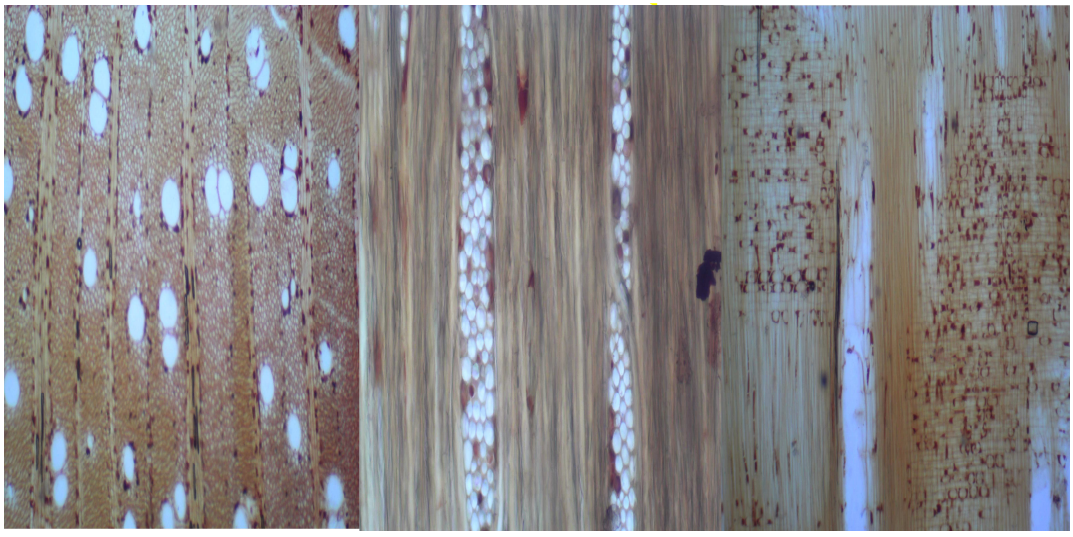

Figure 2: Light microscope images where a. Transverse section (TS); b. Tangential section (TLS); C. Radial section (RLS) of tamarisk wood (*Tamarix sp.* L.) taken from statuette no. 1408

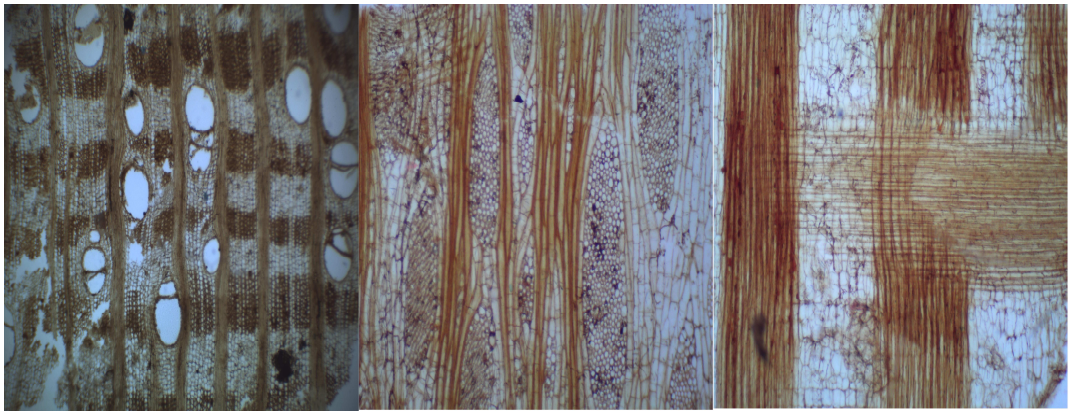

Figure 3: Light microscope images where a. Transverse section (TS); b. Tangential section (TLS); C. Radial section (RLS) of sycamore fig (*Ficus sycomorus*) taken from statuette no. 2213

3.2. SEM–EDX microanalysis

The elemental composition of painted layer samples was identified by the SEM/EDX analysis (Table1 and Figures 4,5,6,7,8,). According to the EDX results, the preparation layer in the statuette no. 1408 was primarily made up of the components C, Ca, S, and O, which indicates that it was most probably composed of a mixture of calcium carbonate and gypsum and the statuette no. 2213 was made with calcium carbonate (17&18). This result is consistent with FTIR analysis.

The elemental composition of the black pigment in the two statuettes contains C, O, Na, Mg, Al, Si, S, and Ca elements. However, there are several differences, such as the presence of chloride element (Cl) in statuette no. 1408 and an increase in the percentage of sodium (Na), which suggests existence of salt efflorescence on the black pigment. Additionally, the fact that Fe and Cu are present indicates that the painter combined and applied pigment leftovers with black pigment in statuette no. 2213. Data from the EDX spectrum showed that the red pigment mostly constituted of the elements C, O, Na, Mg, Al, Si, S, K, Ca, and Fe, with varied percentages for each statuette's red paint layers. This suggests that hematite was employed as a red pigment in both statuettes (19). The gold paint layer on statuette no. 1408 was made up of C, O, S, Ca, and Au components, where Au is the most abundant element in the gold layer. Further evidence suggests that the white pigment is formed of calcium sulphate found in the primary components C, O, S, and Ca of the white pigment in statuette no. 1408. Egyptian blue is the most likely pigment to have been present in this specimen, according to the blue pigments discovered in the EDX pattern from statuette no. 2213, which revealed that this specimen's elemental composition was C, O, Mg, Al, Si, S, Ca, and Cu (20&21). It is important to note that the elements Na, Mg, Al, Si, S, and Ca appear in the majority of paint layers since they were present in the preparation layers for the two statuettes (22&19).

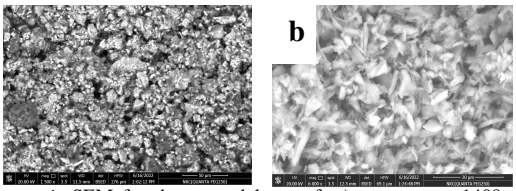

Figure 4: SEM for the ground layer of: a) statuette no.1408; b) statuette no.2213

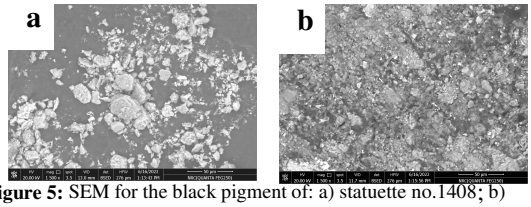

Figure 5: SEM for the black pigment of: a) statuette no.1408; b) statuette no.2213

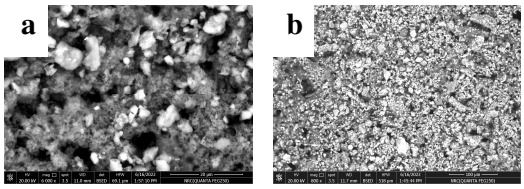

Figure 6: SEM for the red pigment of: a) statuette no.1408; b) statuette no.2213

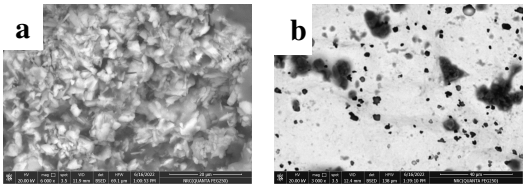

Figure 7: SEM for statuette no.1408; a) the white pigment, b) the gold pigment

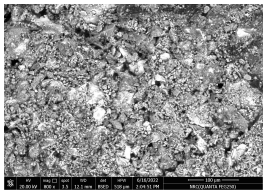

Figure 8: SEM for statuette no.2213 for blue pigment

Table (1)

The elemental analysis (Mean ± SD) of samples of ground layer, black, red pigments from the two wooden statuettes, white and gold from statuette no.1408, and blue pigment from statuette no. 2213

element	Ground layer		Black		Red		White	Gold	Blue
	no 1408	no 2213	no 1408	no 2213	no 1408	no 2213	no 1408	no 1408	no 2213
C	28.83± 1.29	39.50± 0.31	55.857 ± 1.37	38.23± 1.83	48.57± 2.63	42.14± 1.79	52.79± 0.45	40.16± 0.45	54.19± 0.55
O	49.49±0.18	49.88±0.16	36.94±1.57	48.31±1.68	41.88±1.3	47.70±1.87	39.49± 0.24	33.96± 2.69	37.17±0.86
Na	———	———	1.31± 0.24	0.56± 0.13	0.48± 0.05	1.34± 0.27	———	———	———
Ca	12.58± 0.88	10.58± 0.20	0.78± 0.54	4.29± 0.11	2.85± 0.43	1.92± 0.33	4.07± 0.13	2.32± 0.34	2.61± 0.11
Mg	———	———	0.237± 0.06	0.53± 0.03	0.37± 0.01	0.41± 0.05	———	———	0.40± 0.07
Al	———	———	1.54± 1.40	1.24± 0.09	1.26± 0.06	3.96± 0.82	———	———	0.82± 0.04
Si	———	———	1.37± 0.93	5.33± 0.39	2.36± 0.44	3.05± 0.26	———	———	3.44± 0.11
S	9.08± 0.58	———	0.45± 0.04	0.48± 0.13	1.10± 0.07	0.32± 0.05	3.40± 0.16	2.41± 0.19	0.48± 0.13
K	———	———	———	0.16± 0.04	0.21± 0.02	0.17± 0.05	———	———	———
Cl	———	———	0.43± 0.02	———	———	———	———	———	———
Fe	———	———	———	0.43± 0.09	0.46± 0.10	1.11± 0.03	———	———	———
Cu	———	———	———	0.47± 0.06	———	———	———	———	0.90± 0.08
Au	———	———	———	———	———	———	———	21.63± 0.72	———

3.3. FTIR Analysis

In order to identify the binding media in the painted preparation layers of the two statuettes, FTIR was used to investigate the painted layer specimens of the wooden statuettes no.2213 and no.1408 (Figure 9a, b). In the wooden statuette 2213, bands at 1642 cm^{-1} and 1533 cm^{-1} in the FTIR spectrum may be due to the C-O stretching absorption (amide I) and the C-N-H bending absorption (amide II), which are typical protein vibrations indicative of animal glue. In addition, the band at 1411cm^{-1} and 1428 cm^{-1} is attributed to C-H bending band (11&16&23) in wooden statuette no. 1408. The bands of protein from egg in FTIR spectra are assigned as follows: at 2926 and 2856 cm^{-1} to aliphatic C–H stretching groups, at 1582 cm^{-1} to the C–N–H group bending band, and at 1616 cm^{-1} to the carbonyl group (C=O) stretching (24). According to the FTIR analysis of the statuette no. 1408, the small peaks at 669 and 602 cm^{-1} are assigned to the stretching and bending modes of sulphate, characteristic of gypsum, while the bands at 873 cm^{-1} in statuette no. 1408, and the band around 872 cm^{-1} in statuette no. 2213, are characteristic of the C–O stretching mode of carbonate, presumably indicating that the layer is composed of calcium carbonate and gypsum in statuette no. 1408 (25) and calcium carbonate in statuette no.2213.

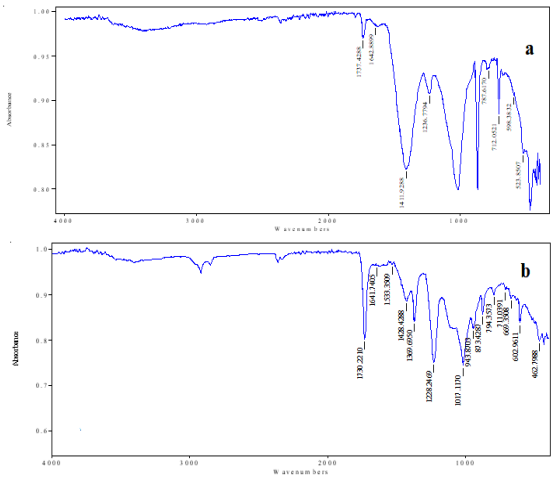

Figure 9 a, b: FTIR spectra of the painted preparation layers of the two wooden statuettes; where (a) for wooden statuette no. 2213 showed that the binding media is animal glue, and (b) wooden statuette no. 1408 showed that the binding media is egg white

3.4. Raman spectroscopy

The Raman results of preparation layers and pigments of the two statuettes show the basic materials that have been commonly identified in ancient Egyptian art. As shown in Figure 10a the Raman spectra of the preparation layers applied on the statuette no. 1408 presented a strong peak at 1008 cm^{-1} that is nearly identical to the symmetric stretching of SO_4 tetrahedra, the peak of gypsum's strongest Raman spectra (26). In the Raman spectra of the preparation layer of statuette no. 2213, the symmetric stretching mode vibration of the carbonate ion present at 1085, 713, 282 and 155 cm^{-1} (Figure 10b) can be attributed to calcite (27&28). The black pigment Raman spectra of the two statuettes were similar (Figure 11a, b). There were two peaks at 1320–1360 and 1500–1600 cm^{-1}. Since the band at 1320–1360 cm^{-1} results from stretching vibrations in the graphite structure and the band at 1500–1600 cm^{-1} appears as a result of defects in the graphite structure and the presence of heteroatoms, this proves that charcoal-based amorphous carbon was used to create the black pigment (26&29&30). The Raman spectra of red pigment in the two statuettes (Figure 12a, b) show peaks occurring at around 288, 419, and 615 cm^{-1} that are attributed to hematite (30&31&32&33&34). The band appeared at around 1323 cm^{-1} (Figure 12b) can be attributed to a burnt organic matter (30&34). Surprisingly, the Raman spectra of white pigment in statuette no.1408 (Figure 13a) suggest that the chemical composition of the white pigment consists basically of a mixture of gypsum (defined by bands at around 186, 411, 616, 654, and 1008 cm^{-1}) and anhydrite (defined by band at around 604 and 672 cm^{-1}) (2&26). As seen in Figure 13b, cuprorivaite, commonly known as Egyptian blue, is the main component of the blue pigment and can be identified by the presence of its characteristic bands at 1079, 553, 371, and 169 cm^{-1} (35). The bands around (1660, 1585, 1550, 1448, 1241, 1207, 1041, 1003, 934, 900, 849, 828, 698, and 622cm^{-1}) showed that the binding media in statuette no.1408, is egg white (36&37).

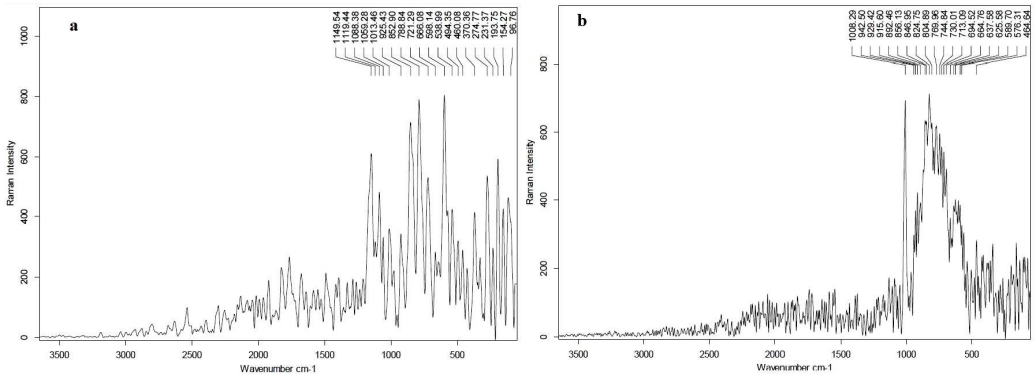

Figure 10: Raman spectra of the paint grounds of the two statuettes, where (a) the statuette no. 2213 and (b) the statuette no. 1408

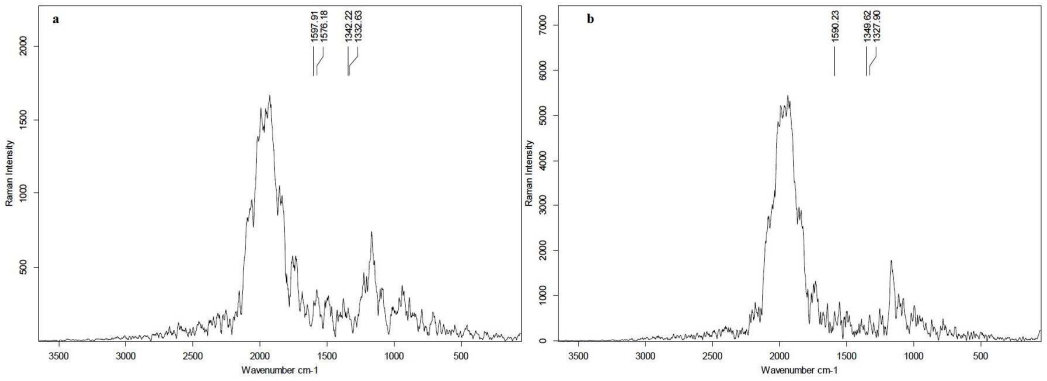

Figure 11: Raman spectra of the black pigment, where (a) the sample from statuette no. 2213 and (b) the sample from statuette no. 1408

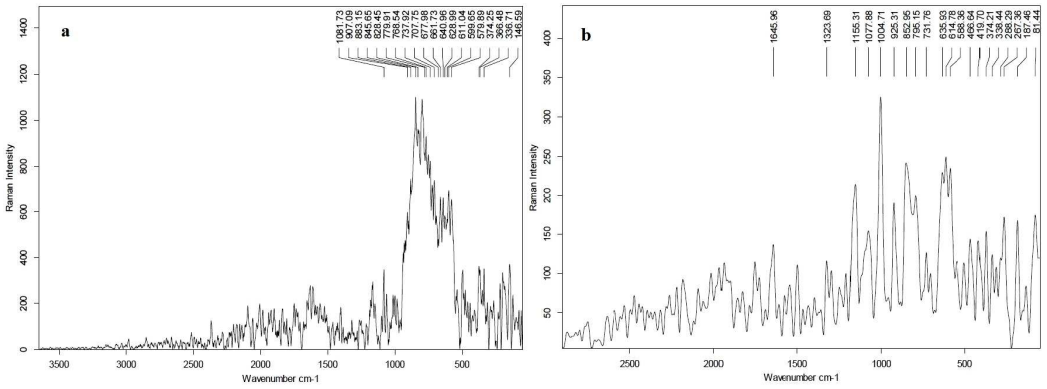

Figure 12: Raman spectra of the red pigment, where (a) the sample from statuette no. 2213 and (b) the sample from statuette no. 1408

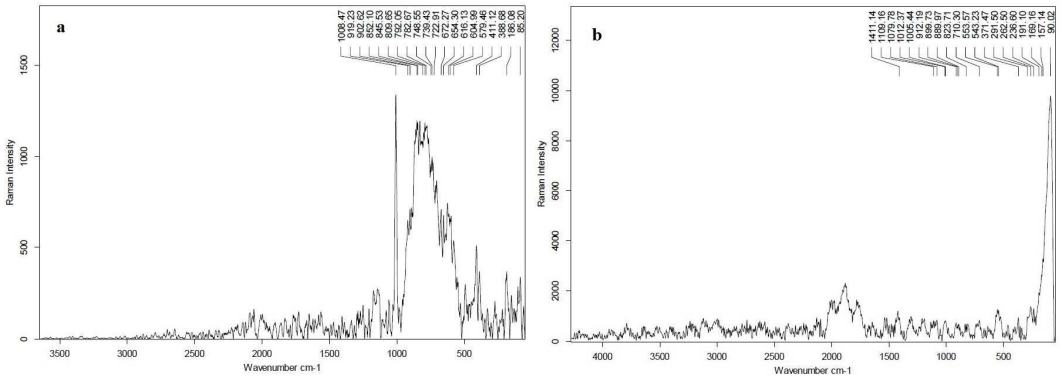

Figure 13: Raman spectra of (a) the white pigment from statuette no. 1408 and (b) the blue pigment from statuette no. 2213

4. Conclusions

The main aim of this study was to characterize preparation layers and pigments from two wooden statuettes of goddess Isis from the Ptolemaic era through multi-analytical techniques such as SEM-EDX and Raman spectroscopy. The wood species utilised in these statuettes were identified using a light microscope (LM). Statuette no. 1408 was carved out of Tamarisk wood (*Tamarix* sp. L.), while statuette no. 2213 was made of sycamore fig (*Ficus sycomorus*); two types of wood very commonly identified in ancient Egyptian artifacts related to burial practices, especially coffins (38). Results from EDX and Raman spectroscopy revealed that the preparation layer for the statuette no. 1408 was predominantly composed of gypsum and calcium carbonate and the statuette no. 2213 was made with calcium carbonate. The binding media in preparation layers and pigments is animal glue, for the statuette no. 2213 and egg white for the statuette no. 1408 according to the FTIR results. EDX coupled with Raman results indicate that hematite was used for the red pigment; an amorphous carbon was used for the black pigment, gypsum was used for the white pigment, gold was used for gilding, and Egyptian blue was used for blue pigment. The pigments found were mostly in accordance with the established ancient Egyptian palette.

5. Conflicts of interest

The authors declare that there is no conflict of interest regarding the publication of this paper.

6. References

[1] Supreme Council of Antiquities' records, Tell Basta,1995.

[2] Ambers, J. (2004). Raman analysis of pigments from the Egyptian Old Kingdom. *Journal of Raman Spectroscopy*, *35*(8 - 9), 768-773 https://doi.org/10.1002/jrs.1187.

[3] Harvey, J. (2009). Wooden Statuary"; In Willeke Wendrich (ed.), UCLA Encyclopedia of Egyptology, Los Angeles, 1-8 http://digital2.library.ucla.edu/viewItem.do?ark=21198/zz001nfbh0

[4] Lucas, A., & Harris, J.R. (1962). Ancient Egyptian Materials and Industries, 4th ed.; Revised and Enlarged by JR Harris. Edward Arnold: London, UK, 1-501.

[5] Marey, M. H. H. (2012). Microanalysis of blue pigments from the Ptolemaic temple of Hathor (Thebes), Upper Egypt: a case study. *Surface and interface analysis*, *44*(9), 1271-1278. https://doi.org/10.1002/sia.4999.

[6] Uda, M., Sassa, S., Yoshimura, S., Kondo, J., Nakamura, M., Ban, Y., & Adachi, H. (2000). Yellow, red and blue pigments from ancient Egyptian palace painted walls. *Nuclear Instruments and Methods in Physics Research Section B: Beam Interactions with Materials and Atoms*, *161*,758-761. https://doi.org/10.1016/S0168-583X(99)00969-6.

[7] Di Stefano, L. M., & Fuchs, R. (2011). Characterisation of the pigments in a Ptolemaic Egyptian Book of the Dead papyrus. *Archaeological and Anthropological Sciences*, *3*, 229-244.

[8] Duce, C., Ghezzi, L., Onor, M., Bonaduce, I., Colombini, M. P., Tine', M. R., & Bramanti, E. (2012). Physico-chemical characterization of protein–pigment interactions in tempera paint reconstructions: casein/cinnabar and albumin/cinnabar. *Analytical and Bioanalytical Chemistry*, *402*(6), 2183-2193. https://doi.org/10.1007/s00216-011-5684-x.

[9] Granzotto, C., & Arslanoglu, J. (2017). Revealing the binding medium of a Roman Egyptian painted mummy shroud. *Journal of Cultural Heritage*, *27*, 170-174, https://doi.org/10.1016/j.culher.2017.04.005.

[10] Badr, N. M., Ali, M. F., El Hadidi, N. M., & Naeem, G. A. (2018). Identification of materials used in a wooden coffin lid covered with composite layers dating back to the Ptolemaic period in Egypt. *Conservar Património*, *29*, 11-24, https://doi.org/10.14568/cp2017029**.**

[11] Derrick, M. R., Stulik, D., & Landry, J. M. (1999). *Infrared spectroscopy in conservation science*. Getty Conservation Institute. Los Angeles, 1-253.

[12] Gale, R., Gasson, P., Hepper, N., Killen, G. (2000). Wood. In: Nicholson, P.T., Shaw, I. (Eds.), Ancient Egyptian Materials and Technology" 15. Cambridge University Press, 334–371.

[13] Wheeler, E.A., Baas, P., Gasson, P.E. (1989). IAWA list of microscopic features for hardwood identification with an appendix on non-anatomical information. *IAWA Bull*, *10*, 219-332.

[14] Cartwright, C., Spaabaek, L. R., & Svoboda, M. (2011). Portrait mummies from Roman Egypt: ongoing collaborative research on wood identification. *British Museum technical research bulletin*, *5*, 49-58.

[15] Crivellaro, A., & Schweingruber, F. H. (2013). *Atlas of wood, bark and pith anatomy of Eastern Mediterranean trees and shrubs: with a special focus on Cyprus*. Springer Science & Business Media, 1-552, https://doi.org/10.1007/978-3-642-37235-3.

[16] Afifi, H., Hamed, S. A. M., Mohamedy, S., & Dawod, M. (2019). A dating approach of a refundable wooden Egyptian coffin lid. *Scientific Culture*, *5*(1), 15-22, https://sci-cult.com/wp-content/uploads/5.1/5_1_2_Afifi-et-al.pdf.

[17] Civici, N., Demko, O., & Clark, R. J. (2005). Identification of pigments used on late 17th century Albanian icons by total reflection X-ray fluorescence and Raman microscopy. *Journal of Cultural Heritage*, *6*(2), 157-164, https://doi.org/10.1016/j.culher.2005.01.002.

[18] Sakr, A. A., Ghaly, M. F., Abdulla, M., Edwards, H. G., & Elbashar, Y. H. (2020). A new light on the grounds, pigments and bindings used in ancient Egyptian cartonnages from Tell Al Sawa, Eastern Delta, Egypt. *Journal of Optics*, *49*(2), 230-247, https://doi.org/10.1007/s12596-020-00612-8.

[19] Mostafa, A. M., Hamed, S. A. E. K. M., Afifi, H., & Mohamady, S. (2019). A comparative study on the color change of pigments due to the consolidation of conventional spectroscopic techniques and laser-induced breakdown spectroscopy. *Applied Physics A*, *125*(8), 1-9, https://doi.org/10.1007/s00339-019-2849-5.

[20] Scott, D. A., Dodd, L. S., Furihata, J., Tanimoto, S., Keeney, J., Schilling, M. R., & Cowan, E. (2004). An ancient Egyptian cartonnage broad collar-Technical examination of pigments and binding media. *Studies in conservation*, *49*(3), 177-192,https://doi.org/10.1179/sic.2004.49.3.177.

[21] Orsega, E. F., Agnoli, F., & Mazzocchin, G. A. (2006). An EPR study on ancient and newly synthesised Egyptian blue. *Talanta*, *68*(3), 831-835, https://doi.org/10.1016/j.talanta.2005.06.001.

[22] Perdikatsis, V & Brecoulaki, H. (2008).The use of red and yellow ochres as painting materials in Ancient Macedonia" In: *Proceedings of the 4th Symposium of the Hellenic Society for Archaeometry*, Facorelis, G, Zacharias, N. and Polikreti, K. (Eds.), Proceedings of the 4th Symposium of the Hellenic Society for Archaeometry. National Hellenic Research Foundation, Athens, 28-31 May 2003, Publisher: Archaeopress British Archaeological Reports, BAR International Series 1746, 559- 567. ISBN: 978 1 4073 0188.

[23] Newman, R & Halpine, S. M. (2001). The binding media of ancient Egyptian painting." Colour and painting in ancient Egypt, 22-32.

[24] Vornicu, N., Bibire, C., Murariu, E., & Ivanov, D. (2013). Analysis of mural paintings using in situ non - invasive XRF, FTIR spectroscopy and optical microscopy. *X - Ray Spectrometry*, *42*(5), 380-387, https://doi.org/10.1002/xrs.2459.

[25] Böke, H., Akkurt, S., Özdemir, S., Göktürk, E. H., & Saltik, E. N. C. (2004). Quantification of $CaCO_3$–$CaSO_3 \cdot 0.5\ H_2O$–$CaSO_4 \cdot\ 2H_2O$ mixtures by FTIR analysis and its ANN model. Materials Letters, 58(5),723-726, https://doi.org/10.1016/j.matlet.2003.07.008.

[26] Moon, D. H., Lee, N. R., & Lee, E. W. (2021). Ancient pigments in Afrasiab murals: characterization by XRD, SEM, and Raman spectroscopy. *Minerals*, *11*(9), 939, 1-11, https://doi.org/10.3390/min11090939.

[27] Soldati, A. L., Jacob, D. E., Wehrmeister, U., & Hofmeister, W. (2008). Structural characterization and chemical composition of aragonite and vaterite in freshwater cultured pearls. *Mineralogical*

Magazine, *72*(2), 579-592, https://doi.org/10.1180/minmag.2008.072.2.579.

[28] https://rruff.info/calcite/display=default/R040070.

[29] Van der Weerd, J., Smith, G. D., Firth, S., & Clark, R. J. (2004). Identification of black pigments on prehistoric Southwest American potsherds by infrared and Raman microscopy. *Journal of Archaeological Science*, *31*(10), 1429-1437, https://doi.org/10.1016/j.jas.2004.03.008.

[30] Gomes, H., Rosina, P., Holakooei, P., Solomon, T., & Vaccaro, C. (2013). Identification of pigments used in rock art paintings in Gode Roriso-Ethiopia using Micro-Raman spectroscopy. *Journal of Archaeological Science*, *40*(11), 4073-4082, https://doi.org/10.1016/j.jas.2013.04.017.

[31] De Faria, D. L., Venâncio Silva, S., & De Oliveira, M. T. (1997). Raman microspectroscopy of some iron oxides and oxyhydroxides. *Journal of Raman spectroscopy*, *28*(11), 873-878, https://doi.org/10.1002/(SICI)1097-4555(199711)28:11<873::AID-JRS177>3.0.CO;2-B.

[32] Clark, R. J., & Curri, M. L. (1998). The identification by Raman microscopy and X-ray diffraction of iron-oxide pigments and of the red pigments found on Italian pottery fragments. *Journal of Molecular Structure*, *440*(1-3), 105-111, https://doi.org/10.1016/S0022-2860(97)00239-1.

[33] Cornell, R. M., & Schwertmann, U. (2003). *The iron oxides: structure, properties, reactions, occurrences, and uses* (Vol. 664). Weinheim: Wiley-vch, https://doi.org/10.1515/CORRREV.1997.15.3-4.533

[34] Hanesch, M. (2009). Raman spectroscopy of iron oxides and (oxy) hydroxides at low laser power and possible applications in environmental magnetic studies. *Geophysical Journal International*, *177*(3),941-948, https://doi.org/10.1111/j.1365-246X.2009.04122.x.

[35] Edwards, H. G., Jorge Villar, S. E., & Eremin, K. A. (2004). Raman spectroscopic analysis of pigments from dynastic Egyptian funerary artefacts. *Journal of Raman spectroscopy*, *35*(8 - 9),786-795,https://doi.org/10.1002/jrs.1187.

[36] Osticioli, I., Nevin, A., Anglos, D., Burnstock, A., Cather, S., Becucci, M., & Castellucci, E. (2008). Micro - Raman and fluorescence spectroscopy for the assessment of the effects of the exposure to light on films of egg white and egg yolk. *Journal of Raman Spectroscopy: An International Journal for Original Work in all Aspects of Raman Spectroscopy, Including Higher Order Processes, and also Brillouin and Rayleigh Scattering*, *39*(2),307-313, https://doi.org/10.1002/jrs.1915.

[37] Vandenabeele, P., Wehling, B., Moens, L., Edwards, H., De Reu, M., & Van Hooydonk, G. (2000). Analysis with micro-Raman spectroscopy of natural organic binding media and varnishes used in art. *Analytica Chimica Acta*, *407*(1-2), 261-274, http://hdl.handle.net/1854/LU-124807

[38] El Hadidi, N. M. (2015). Changing research trends in the field of archaeological wood at the Conservation Department, Faculty of Archaeology, Cairo University. *Studies in Conservation*, *60*(3),143-154, https://doi.org/10.1179/2047058413Y.0000000124